Self-Organized Criticality: On Generalized Sandpile Models

Wenrui Yuan

November 4, 2020

Abstract

Self-Organized Crticality is concept that non-dynamical systems with extended degree of freedom follow power-law behavior. As the archetype of this concept, sandpile models have been studied under different settings, numerically or theoretically. In this report, we study three types of sandpile models to understand how different toppling rules render unique behavior for each of them. Finally, we will discuss techniques that can help us to establish a more precise model in simulating the sandpile dynamics .

1 Introduction

Self-Organized Criticality (SOC) was first introduced by Bak, Tang and Wiesenfeld in 1987 to explain the $1/f$ noise [1]. It was first interpreted as a non-equilibrium dynamical system at slowly driving steady state, with long range spatial and temporal correlations and extended degrees of freedom, that is not controlled by predefined methods or parameters. In [1, 2], they studied the cascading effect of small perturbations on a structure of minimally stable through a simple abelian sandpile model that exhibits the power-law behavior. The sandpile model was further investigated through simulation in presenting the temporal and spatial correlations and thus identifying the $1/f$ noise [2], and scaling invariance allows the study of extended dynamical systems on power-law spectrum [17]. The sandpile model was generalized by Chau and Cheng through establishing the fundamental model, rendering the device for creating sandpile models that obeys critical exponent correlations [3]. Other models, although showing the power-law distributions, whose results often deviate from the original sandpile model, demand studies in more generalized context[12, 7]. Critical slope models were studied and believed to be non-abelian due to non commutative toppling configurations and disagreement in simulation results with general abelian models [15, 11].

In this report, we will examine three types of sandpile models in the context of extended dynamical system. The main purpose is to compare simulation results from different models and thus further generalize our model to simulate more realistic avalanching dynamics.

Structures of this report is as follows: section 2 will cover models and implementation methods, where arguments are mainly focused on the general abelian sandpile as for its mathematical soundness. Section 3 will be primarily simulation results under different constraints, followed by conclusions and discussion in section 4.

2 Models and Methods

Before defining the actual model, it is important understand correlations between phenomena that follow power-law distribution and scale invariance, which is often defined under a class of functions

$$f(\lambda x) = C(\lambda) f(x),$$

where λ is the scaling factor. One example is monomials, $f(x) = x^n$, which follows

$$f(\lambda x) = (\lambda x)^n = \lambda^n x^n,$$

where λ^n is the scaling exponent with degree n. Hence, the power-law function of the form $f(x) = ax^k$ can be applied to describe a wide range of dynamical systems that exhibit scale invariance.

2.1 Abelian sandpile model

For a initially empty, finite size surface, if we add a grain of sand randomly per unit time, then sand grains will accumulate until a certain critical state, where grains start to fall off. In reality, one would expect such a behavior does not change even on a sufficient large finite size surface, which is equivalent to scale invariance: if a local perturbation (i.e. a drop of sand) is introduced to the minimally stable system, then the system becomes unstable, triggering more avalanches that can no longer described by the local dynamics. In words, the sandpile is self-governed, and critical state is only determined by the exponent.

Another important aspect of this model is the restriction of finite size; suppose instead that a infinite size surface is given, what is the relaxation time for this system? Or, if the initial empty assumption is given, how long would it take to cause an avalanche? Although studies have ensured convergence with the latter configuration, it is highly subject to initial conditions [16, 10].

2.1.1 Bak-Tang-Wiesenfeld model

The original model in 2D was defined on a empty flat surface [2]. In particular, our implementation considers a $N \times M$ grid and let $p_t(i,j)$ be the number of grains at site (i,j) for each unit time $t \in \mathbb{N}^0$. Assume the surface is empty for now, then adding a grain of sand is defined as:

$$p_t(i,j) = p_t(i,j) + 1.$$

If grains on a single site exceed the critical value, p_c, then a topple is defined as distribute sands to neighbouring sites. In particular, if $p_c = 4$, then for any site $p_t(i,j) \geq 4$, the topping rule can be defined as

$$\begin{aligned} p_t(i,j) &= p_t(i,j) - 4, \\ p_t(i \pm 1, j) &= p_t(i \pm 1, j) + 1, \\ p_t(i, j \pm 1) &= p_t(i, j \pm 1) + 1. \end{aligned} \tag{1}$$

Our implementation further assume an open boundary condition is placed, so that grains may fall of the edge. Hence, it is expected the system drives toward a steady state where grains added equal to the grains falling off the edge. Here, one should not confuse a steady state with an equilibrium: an equilibrium often describes a closed system with no driving force, whereas a steady state is associated with open systems, where net change over time is zero. This led us to believe that the system drives toward a stationary state where observables are independent of time, as suggested in previous studies [5]. Illustration of (1) in a single avalanching event can be found in figure 1. An avalanche can be defined as recurrent operations of (1) until $p_t(i,j) \leq 4$, $\forall\, i \in \{1, \cdots, N\}, j \in \{1, \cdots, M\}$. In this case, one can say that a height configuration at any stationary states is a recursion of its previous stationary state. At stationary state, or in a more general context, steady state, avalanche stops and the model will exhibit power-law behavior in metrics like cluster size and duration, as discussed in [1, 2].

We believe that, at steady state, energy inflow (adding grains) and outflow (grains falling off boundary) should be equal. Therefore, the average height of the grid, defined by

$$\langle p_t \rangle := \frac{1}{NM} \sum_{i,j} p_t(i,j), \tag{2}$$

is approximately 2.

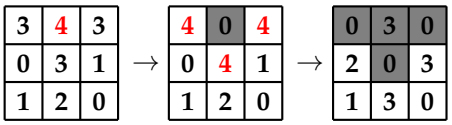

Figure 1: Single avalanche of the model under abelian toppling rules on a 3×3 grid. The avalanche has a size of 4 and duration of 2.

To further study the avalanche, we will be focusing on the following properties:

Size (s): the number of topples required for the system to relax.

Area (s_d): distinct sites toppled

Loss (l): the number of grains fell off the grid.

Length (ℓ): maximal L^1 distance from the first toppled site

As stated in the original paper [2, 1], frequency distribution of avalanche size s in log-log scale should follow:

$$D(s) \approx s^{-\tau}, \quad \tau \approx 1. \tag{3}$$

We argue that the avalanche area, which is equivalent to the number of distinct topples, s_d, should also follow (3). Unlike avalanche size and area, which are both observable from the system, avalanche loss and length are measures primarily for describing the state of particles (grains), we therefore expect them not to follow (3). Instead, to measure all four properties using a single functional form, let

$$D(\mathbf{x}) \approx a\mathbf{x}^{-k},$$

be defined as the frequency distribution of $\mathbf{x} \in \{s, s_d, l, \ell\}$. We intentionally let the length be defined as the L^1 distance as the topple dynamics shown in figure 1 has no diagonal movement. Further discussion on this argument and correlation between these properties will be covered in later sections. Intuitively, avalanche loss is closely related to energy loss in many cases and were used interchangeably by many. In general, a sandpile model that allows energy loss is called a dissipative sandpile model. We believe that the dissipative sandpile model is ergodic, that is, ensemble average is equal to the time average, given the time indpendent nature of this model [9].

2.1.2 Abelian property

One of the aspect that distinctify abelian models with other SOC models is the abelian property. That is, it allows commutative unstable configuration: if there are more than one unstable sites, then one toppling will commute with others (i.e. order does not matter). To show this, let $\Delta(\mathbf{x}, \mathbf{y})$ be the toppling matrix, satisfying the following conditions

$$\forall\, \mathbf{x} \neq \mathbf{y} \in L, \quad \Delta(\mathbf{x}, \mathbf{y}) = \Delta(\mathbf{y}, \mathbf{x}) \geq 0, \tag{4a}$$

$$\forall\, \mathbf{x} \in L, \quad \Delta(\mathbf{x}, \mathbf{x}) < 0, \tag{4b}$$

$$\forall\, \mathbf{x} \in L, \quad \sum_{\mathbf{y} \in L} \Delta(\mathbf{x}, \mathbf{y}) \leq 0, \tag{4c}$$

$$\sum_{\mathbf{x}, \mathbf{y} \in L} \Delta(\mathbf{x}, \mathbf{y}) < 0. \tag{4d}$$

(4a) simply implies the commutativity of unstable configurations. This is indeed important, otherwise one need to keep track of all unstable sites for every single avalanches since toppling of a unstable site may cause other unstable sites to return to stable under non-commutative configurations. Together with (4b), this ensures that only toppled sites lose grains but not other sites $\mathbf{x} \neq \mathbf{y}$, which is important as one need to make sure there is no energy created inside each toppling processes. (4c) and (4d) combined simply shows that grains may fall of the edge, as stated in the open boundary requirement. In fact, some have argued that a steady state is not possible for a closed one [4]. Now, if (4) are satisfied, then the toppling rule can be defined by

$$\Delta(\mathbf{x}, \mathbf{y}) = \begin{cases} -2d & \mathbf{x} = \mathbf{y} \\ 1 & \mathbf{x}, \mathbf{y} \text{ are nearest neighbors} \\ 0 & \text{otherwise} \end{cases}, \tag{5}$$

where d denotes the dimension. Clearly, in 2D models (i.e. $d = 2$), (5) implies that $\Delta(\mathbf{x}, \mathbf{x}) = -4 = -p_c$, which is the same as the critical height for a site to topple as discussed in 2.1.1. If we put

$$p(\mathbf{x}) = p(\mathbf{x}) + \Delta(\mathbf{x}, \mathbf{x}), \tag{6}$$

where $p(\mathbf{x})$ denotes the height configuration at site $\mathbf{x}$. Then it is the same as previously defined toppling rules in (1), where (4a) and (4b) are clearly satisfied. With (5), we may show that (6) can be generalized to

$$(T_{\mathbf{x}} p)(\mathbf{y}) := \begin{cases} p(\mathbf{y}) + \Delta(\mathbf{x}, \mathbf{y}) & p(\mathbf{x}) \geq \Delta(\mathbf{x}, \mathbf{x}) \\ p(\mathbf{y}) & \text{otherwise} \end{cases}, \tag{7}$$

where $T_{\mathbf{x}}$ is the toppling operator associated with adding a grain at site $\mathbf{x}$. To satisfy commutativity as discussed earlier, we want to show that

$$(T_{\mathbf{x}} \circ T'_{\mathbf{x}})(p) = (T'_{\mathbf{x}} \circ T_{\mathbf{x}})(p). \tag{8}$$

Write the LHS by directly applying (7):

$$(T_{\mathbf{x}} \circ T'_{\mathbf{x}})(p) = \begin{cases} p(\mathbf{y}) + \Delta(\mathbf{x},\mathbf{y}) + \Delta(\mathbf{x}',\mathbf{y}) & p(\mathbf{x}) \geq \Delta(\mathbf{x},\mathbf{x}) \text{ and } p'(\mathbf{x}') \geq \Delta(\mathbf{x}',\mathbf{x}') \\ p(\mathbf{y}) + \Delta(\mathbf{x},\mathbf{y}) & p(\mathbf{x}) \geq \Delta(\mathbf{x},\mathbf{x}) \text{ only} \\ p(\mathbf{y}) + \Delta(\mathbf{x}',\mathbf{y}) & p'(\mathbf{x}) \geq \Delta(\mathbf{x}',\mathbf{x}') \text{ only} \\ p(\mathbf{y}) & \text{otherwise} \end{cases}$$

Observe that RHS of (8) is the same as the above given the same configuration $p(\mathbf{y})$, with the only difference in the toppling order $p(\mathbf{y}) + \Delta(\mathbf{x}',\mathbf{y}) + \Delta(\mathbf{x},\mathbf{y})$. According to the toppling rule defined in (5), it is obvious that (8) hold.

In general, (8) can describe an avalanche, by introducing the stabilization operator,

$$\mathbb{T} : U_L \to S_L,$$

where U_L is the space of all possible height configurations and $S_L \subset U_L$ is the space of stable height configurations; such an operator can be defined by

$$\mathbb{T} = \prod_{i=1}^{N} T_{\mathbf{x}_i} \tag{9}$$

To show that (9) is well-defined, consider two sequences of vertices

$$\mathbf{x}_1, \mathbf{x}_2, \cdots, \mathbf{x}_n,$$
$$\mathbf{y}_1, \mathbf{y}_2, \cdots, \mathbf{y}_m,$$

that are both stabilizing sequence of p, describing series of (possible) toppling events. If p is stable, then $n = m = 0$; if p is unstable, then $\mathbf{x}_j$ must be somewhere in the $\mathbf{y}_1, \mathbf{y}_2, \cdots, \mathbf{y}_m$ sequence according to (8). Without loss of generality, assume that $j = 1$, so that $\mathbf{x}_1 = \mathbf{y}_i$, for some $1 \leq i \leq m$. Further assume that i is the smallest index, then by (8), it follows that

$$\begin{aligned} (T_{\mathbf{x}_1} T_{\mathbf{y}_{i-1}} \cdots T_{\mathbf{y}_1})(p) &= (T_{\mathbf{y}_{i-1}} T_{\mathbf{x}_1} T_{\mathbf{y}_{i-2}} \cdots T_{\mathbf{y}_1})(p) \\ &\vdots \\ &= (T_{\mathbf{y}_{i-1}} \cdots T_{\mathbf{y}_1} T_{\mathbf{x}_1})(p), \end{aligned}$$

which suffices to show that the sequence

$$\mathbf{x}_1, \mathbf{y}_1, \cdots, \mathbf{y}_{i-1}, \mathbf{y}_{i+1} \cdots \mathbf{y}_m$$

is also a stabilizing sequence of p. Therefore for any configuration p, the stabilizing operator $\mathbb{T}p = p'$ is unique, and therefore well defined.

2.2 Stochastic sandpile model

In general, stochastic sandpile models are variants which exhibit stochastic behavior, or in simple terms, randomness. Although there has been dispute on the exact definition, it was believed that the manna model was the first implementation [12]. Later studies have shown some abelian properties of this model [6, 14], yet disagreed by others [15]. Our implementation is defined on the same basis as discussed in 2.1.2 with a stochastic toppling rules. That is, whenever $p_t(i,j) \geq 4$, it follows that

$$p_t(i,j) = p_t(i,j) - 4$$

where 4 of the neighboring sites of (i,j) are randomly selected form 8 neighbors $(i \pm 1, j \pm 1)$ with certain probability. Immediately, we may observe that (5) is satisfied if we assume that all 8 neighbors are now considered as nearest neighbors of $\mathbf{x}$. Although showing some abelianity, many have

suggested that this type of model belongs to the universality class [5, 15]. We will not go through these arguments but focus on the same properties which characterize a sandpile model. That is, we are interested in the avalanche size, area, loss and length as well as their correspondence in showing power-law distribution.

Implementation of this model follows the same pipeline as abelian models, except for each toppling at $p(\mathbf{x})$, its neighbors, $\mathbf{y}$, are randomly selected. The probability of each neighboring sites being chose is assumed to be the same in later experiments as our focus is to compare different models but not study a particular one.

2.3 Non-abelian sandpile model

By definition, non-abelian groups fail to satisfy commutativity. Therefore, models that fail to satisfy (4a) can be classified as a non-abelian sandpile model. We have already shown the importance of commutativity, and argued that it is impossible to record an avalanche if there are multiple stabilizing configurations.

In particular, our implementation is similar to the directed slope and critical slope method [13, 11], where we consider slopes measured from neighboring sites. Let p_c be local height threshold, if any of the four instability conditions:

$$\begin{aligned} p_t(i,j) - p_t(i+1,j) &\geq p_c, \\ p_t(i,j) - p_t(i-1,j) &\geq p_c, \\ p_t(i,j) - p_t(i,j+1) &\geq p_c, \\ p_t(i,j) - p_t(i,j-1) &\geq p_c, \end{aligned} \tag{10}$$

is satisfied, then the site will topple, defined by

$$\begin{aligned} p_t(i,j) &= p_t(i,j) - p_c, \\ p_t(i \pm 1,j) &= p_t(i \pm 1,j) + 1, \\ p_t(i,j \pm 1) &= p_t(i,j \pm 1) + 1. \end{aligned} \tag{11}$$

Initially, (11) seems to follow a similar toppling scheme as (1). However, given the instability condition, one should notice that steady state can also be achieved by adding grains of sand. Suppose there are initially two unstable sites, relatively close to each other so that some neighbors are shared. Clearly, if one site toppled and grains are distributed to neighboring sites, the other unstable may become stable without toppling as one of the instability conditions may break. Illustration of non-abelian topple rule can be found in figure 2, where we can see two non-commutative stabilizing sequences are exclusive to each other.

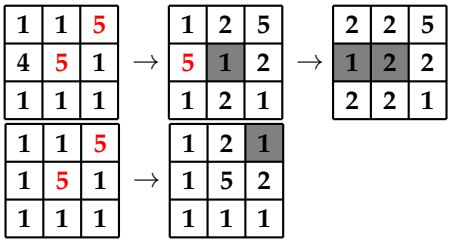

Figure 2: Single avalanche of the critical slope model on a 3×3 grid. Two unstable configurations cause non-commutative stabilizing sequences with different avalanching statistics

We notice that this model is in its nature less stable than other variants as introduction of a single sand can effect multiple sites. To be more specific, adding a grain of sand can change local gradients of all adjacent site. If there more gradient measures are taken near a single site, then it will be more likely for it to satisfy any of the instability conditions, thus leading to an avalanche. Therefore, we think this gradient-based model is a more realistic model in simulating the sand slide dynamics. Implementing a model that consider all possible stabilizing sequences can be hard, or even impossible once the grid gets sufficiently large. Here we introduce a stochastic implementation similar to the stochastic toppling rules shown in 2.2. In particular, the model can be simplified into following procedures:

i. Look for sites that satisfy any of (10), record these sites with different sequences based on which slope measure is taking.

ii. Choose one from all available sequences randomly, and topple them. Because no adjacent sites can be both unstable under the same slope measure, stabilizing one does not break the instability of other.

iii. Repeat i. and ii. until no sites are unstable.

Note that (11) can be generalized by changing the slope measures in (10). For example, some have proposed a variant with only $p_t(i,j) - p_t(i,j+1)$ and $p_t(i,j) - p_t(i+1,j+1)$ are measured [13]. We may think of slope measure as the surface is directed toward that specific direction, which gives sandpiles from the above model a pyramid-like shape [11]. We argue that the threshold for instability p_c must be greater than or equal to the number of slope measures. Otherwise, a hole will form and the avalanche never stops since the unstable sites keep distributing grains even when they reach negative height. This can be visualized as hole-digging process [11]; yet, as the avalanche does not terminate and the model will not reach a steady state, no useful statistics can be collected.

2.4 Implementation method

Every model discussed earlier will be placed on a $N \times M$ grid, initially empty or randomly filled with grains and set to relax. In particular, three types of grain addition at each unit time will be considered: drop at a random site, a specific site and randomly drop around a specific site that follows Gaussian distribution.

Recall that all models are placed in a open system. A "standard" approach to solve boundary conditions involves multiple branching (conditional) statements, which requires heavy computation forces for each avalanche once the simulation grid gets sufficiently large. Hence, we introduce a simulation boundary (padding) that surrounds the grid, so that grains fell on the simulation boundary are counted as lost. Meanwhile, the value from each site on this boundary is reset to zero after a single avalanche is terminated, so that it would not introduce any new unstable sites. We note that this boundary is not only helpful when collecting energy loss, but also allows more complex dynamics by adjusting the size of boundary, .

3 Computational Results

We will begin this section by showing some generic results in proving previous hypothesis and justification. We argued that the average height of sandpile models should be approximately 2, which is true as shown in figure 3; an agreement to a proven result, 17/8, in [8].

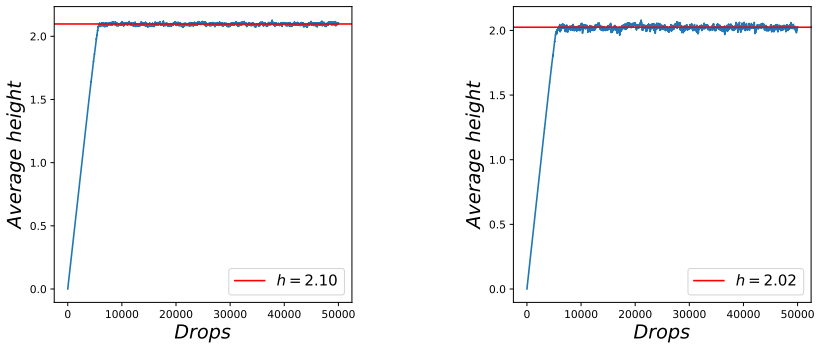

(a) abelian sandpile model (b) stochastic sandpile model

Figure 3: Average height of sandpile models over 5×10^4 drops on 50×50 grid

We have also argued that L^1 norm is a better description of avalanche lengths based on the specific dynamics of our models. This is indeed true if we look at the results shown in figure 4. Although both figures suggest good power-law fits, there are more noises in L^2 distance, due to the squared error.

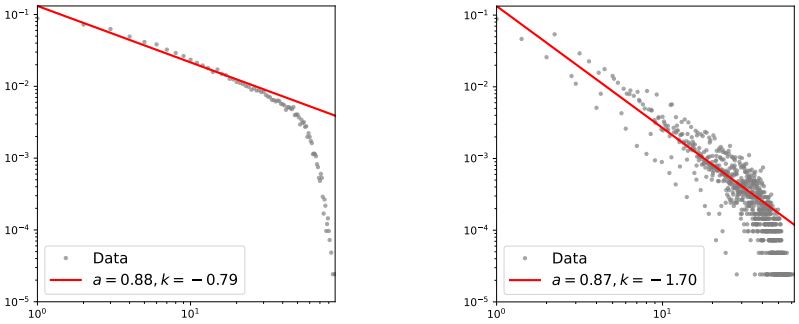

(a) L^1 (b) L^2

Figure 4: Avalanche lengths as (a) L^1 norm and (b) L^2 norm

3.1 Abelian sandpile model

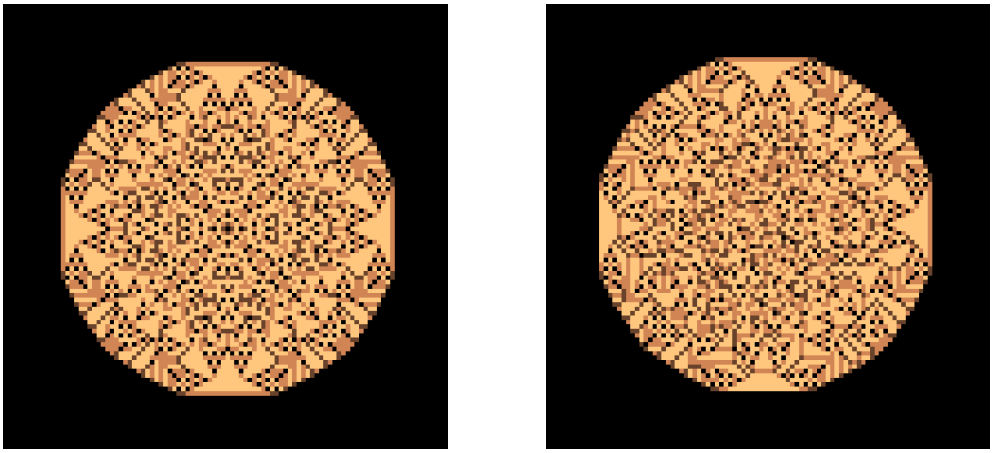

(a) 10^4 grains continuously dropped at the center

(b) 10^4 grains normally distributed near the center

Figure 5: Scale-invariant patterns of the abelian sandpile model on a 100×100 grid

Figure 6 in general displays a relatively convincing power-law behavior, as indicated by the critical exponent marked in red; finite size cutoff is also observed, as suggested by previous studies [11, 2, 7]. The figure also verifies our previous assumptions that critical exponents characterizing avalanche loss and length does not equal ones from avalanche size and area. They are in nature associated with particle dissipation and travel distance, respectively. In particular, we observe that figure 6a and 6c share a similar critical exponent result, $k \approx 1$, for both s and s_d, a good agreement with [2]. On the other hand, profiles in figure 6b all show humps near the cutoff, which is further confirmed by 6c, where introduction of stochasticity yields a more compact distribution near the fitting line. Use figure 5 , we argue that continuous drops at a specific site is the same as a normal distribution of drops near that site, which yields the same dynamics that translates to a slightly organized avalanche pattern (fractal-like, as shown in figure 5), where the heavy-tailedness is amplified, exhibiting a hump-like shape. We call this a "centralized" effect, where most avalanche data are clustered to some specific values due a centralized inflow of energy near a specific point in the spatial domain, as shown in plots of avalanche area distribution.

3.2 Stochastic sandpile model

In general, distribution of s and s_d collected from the stochastic variant share a similar critical exponent result, $k \approx 1.2$, under all dropping configurations. By comparing figure 6 and 7, we notice that distributions for each of $\{s, s_d, l, \ell\}$ under same dropping configuration are very similar across these 2

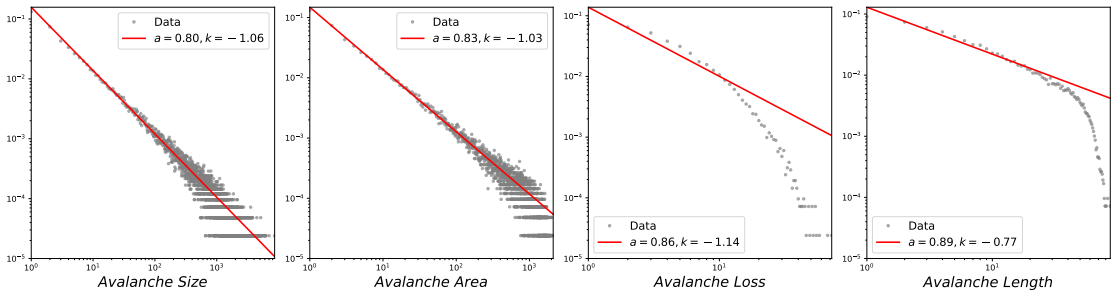

(a) Random drops

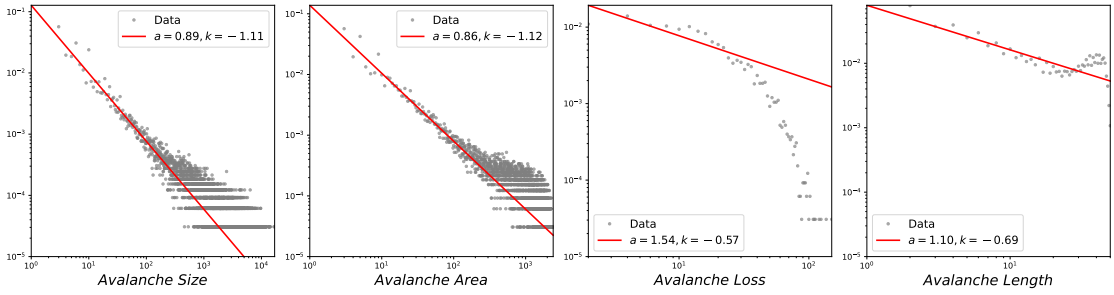

(b) Continuous drops at the center of the grid

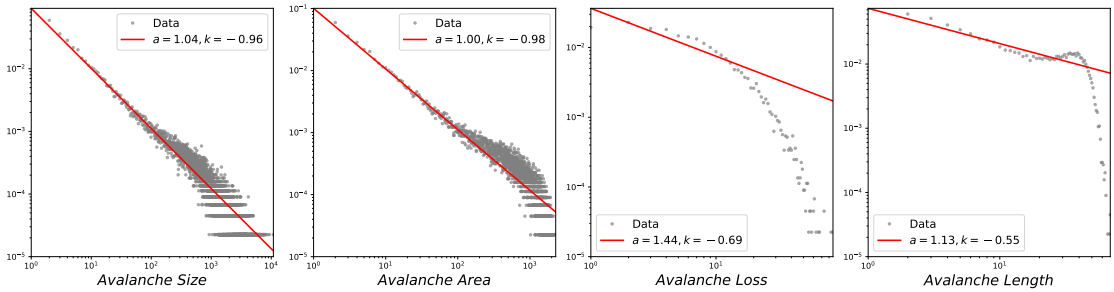

(c) Normally distributed near the center of the grid ($\mathcal{N}\{(25, 25), 5\}$)

Figure 6: Frequency distribution of statisitics in double logarithmic scale; collected from abelian sandpile model with 10^5 grains dropped on a 50×50 grid; distribution ordered from first to last column: $\{s, s_d, l, \ell\}$

models. Moreover, figure 7b and 7c confirm that dropping near (or at) a specific site does introduce a hump-like shape near the cutoff, due to the centralized effect.

3.3 Non-abelian sandpile model

In earlier sections, we discussed the motivation of this model. That is, a directed slope model whose instability is introduced by local gradient, as shown in figure 8. In particular, figure 8a represents the dynamics of a sand slide on a sloped surface whereas figure 8b shows the sand pile on a pyramid. We observe that grains near the boundary are of less height because they may fall off and less likely to accumulate, corresponding to the fact that grains on the boundary of a sloped surface tend to get pushed off by other as suggested by many practical experiments.

This model also allows a more realistic avalanching dynamcis shown in figure . By comparing figure 8b and , we can see that, regardless of the sand dropping scheme, all of them drive to a similar limiting-shape; not so surprising if we compare it with the sand slide dynamics in reality.

For avalanching statistics shown in figure 9, only 9a shows an overall agreement to previous results. We found that distribution for s and s_d in figure 9a are particularly similar to ones in figure 6a. In fact, they both share a critical exponent $k \approx 1$, unlike what some studies have suggested [11, 13]. We believe that this discrepancy is caused by a combination of finite size scaling effect and implementation method. Uncharacteristic behaviors are observed in both figure 9b and 9c. The amount of outliers in distribution plots of avalanche size and area suggest remarkable heavy-tailedness. In 3.1, we have shown that dropping near a specific site increases heavy-tailedness, thus generates humps

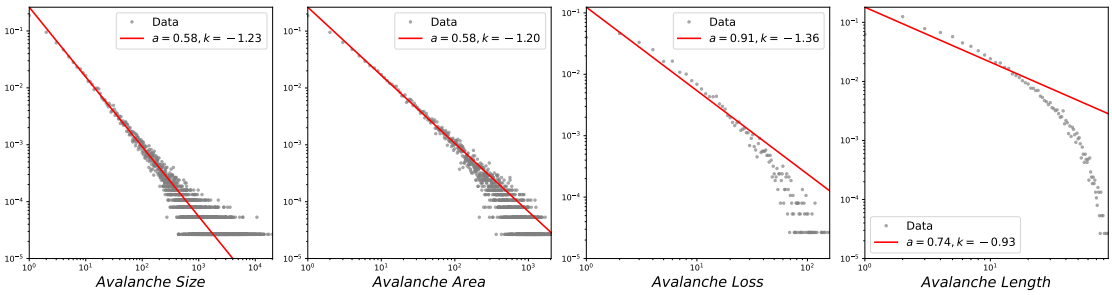

(a) Random drops

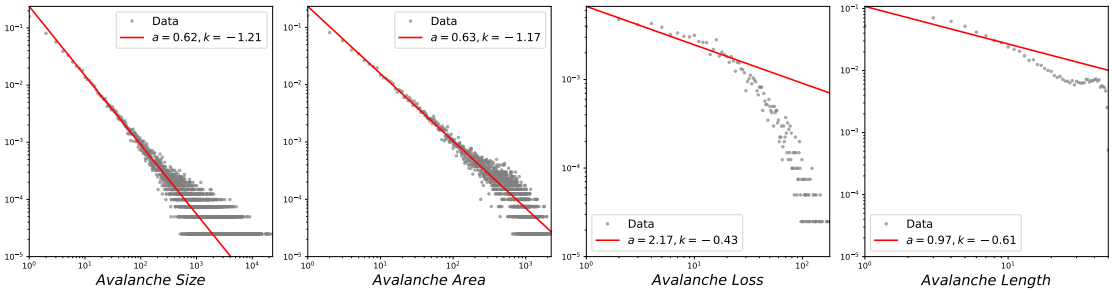

(b) Continuous drops at the center of the grid

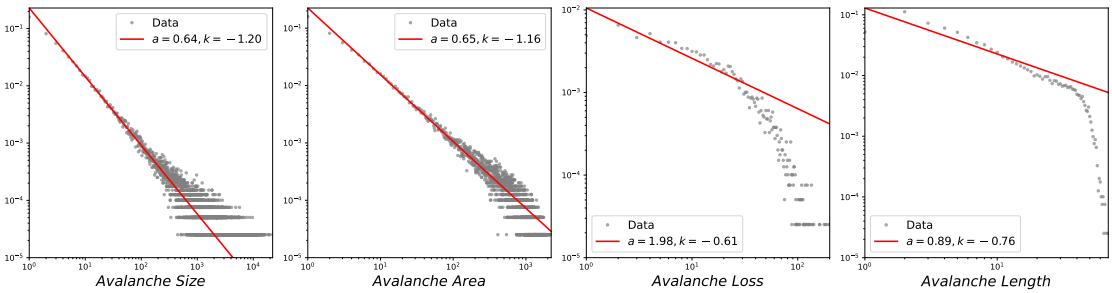

(c) Normally distributed near the center of the grid ($\mathcal{N}\{(25,25),5\}$)

Figure 7: Frequency distribution of statisitics in double logarithmic scale; collected from stochastic sandpile model with 10^5 grains dropped on a 50×50 grid; distribution ordered from first to last column: $\{s, s_d, l, \ell\}$

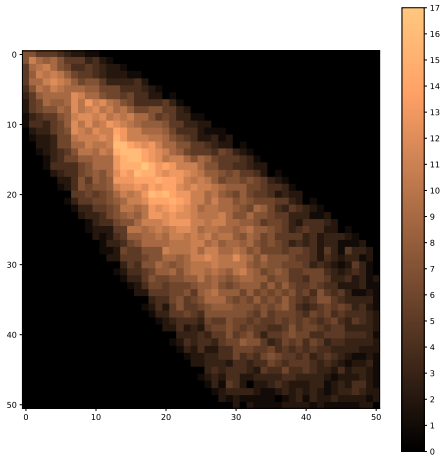

(a) Slopes measured at $p_t(i,j) - p_t(i,j+1)$ and $p_t(i,j) - p_t(i+1,j+1)$; 10^5 drops at $(0,0)$

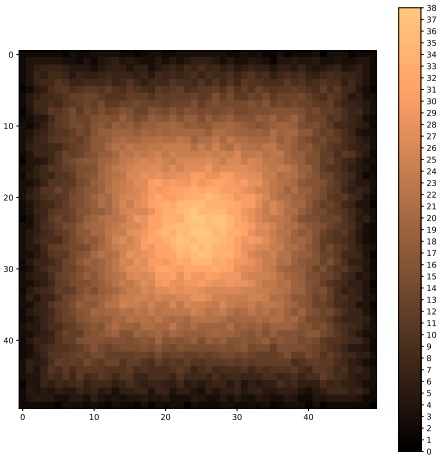

(b) Slopes measured at $p_t(i,j) - p_t(i+1,j), p_t(i,j) - p_t(i-1,j), p_t(i,j) - p_t(i,j+1)$ and $p_t(i,j) - p_t(i,j-1)$; 10^5 drops at $(25,25)$

Figure 8: Visualization of avalanches of non-abelian sandpile model on a 50×50 grid

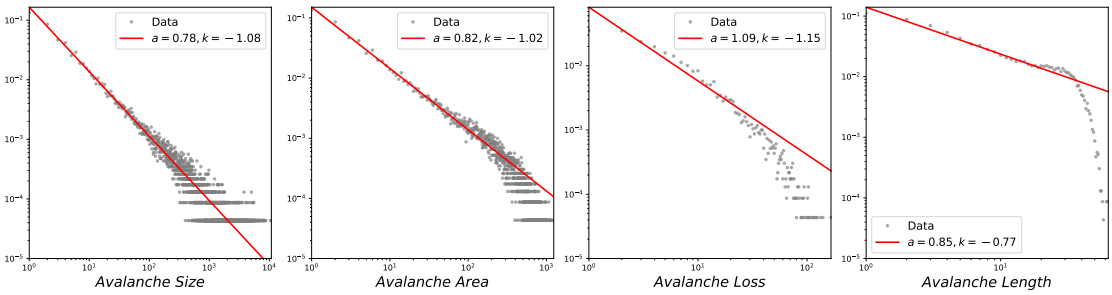

(a) Random drops

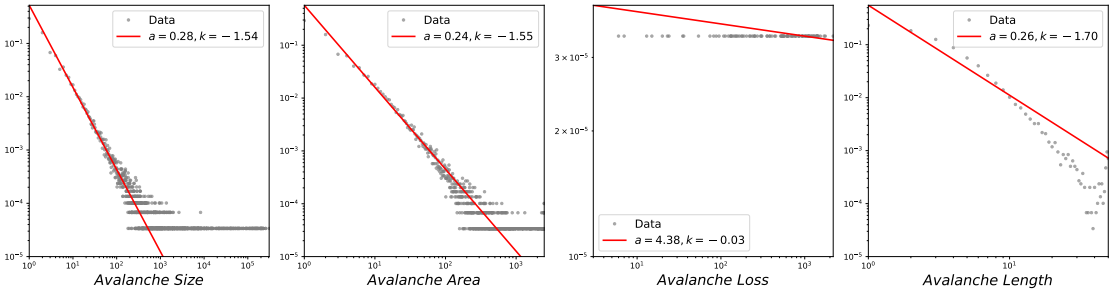

(b) Continuous drops at the center of the grid

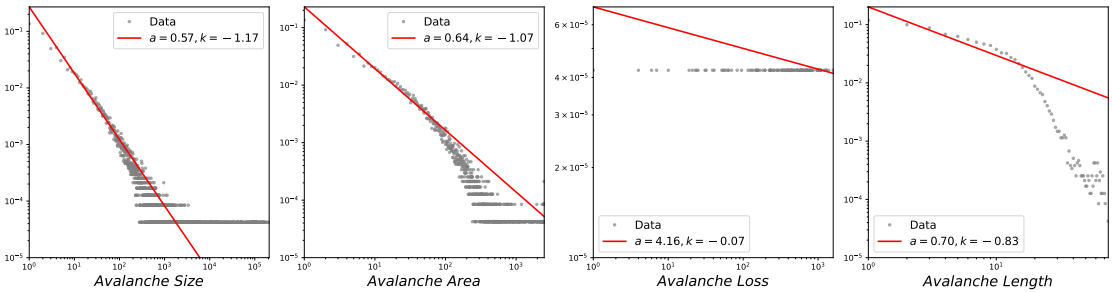

(c) Normally distributed near the center of the grid ($\mathcal{N}\{(25, 25), 5\}$)

Figure 9: Frequency distribution of statisitics in double logarithmic scale; collected from non-abelian sandpile model with 10^5 grains dropped on a 50×50 grid; distribution ordered from first to last column: $\{s, s_d, l, \ell\}$

in distribution plots, which holds for this model as well, where the hump is translated to even larger avalanches. As discussed earlier, a sandpile model defined with gradient-based toppling rule is in its nature less stable than the other variants since the addition of a single grain of sand could change local gradient significantly. Coupled with the centralized effect of sand drops, later recursions find significantly large avalanches ($s > 10^5$), indicating a collapse of sand from the center. For avalanche loss distributions, we observe that a great amount of sand grains were lost throughout the relaxation, which is indeed true considering abnormal avalanche sizes.

4 Conclusion and Discussion

In this report, we studied three types of sandpile model and their characteristics by carefully examining related works and simulation results. The overall power-law behavior for all models are ensured, but strong disagreement in critical exponents collected across different models suggest that they are belong to different problem classes. In general, results of avalanche size and area are shown to be true by previous studies; yet the lack of detailed study on loss and length questions the validity of our results. On the other hand, practicality of the stochastic implementation of critical slope model in emulating sand slide dynamics has been shown.

References

[1] P. Bak, C. Tang, and K. Wiesenfeld. Self-organized criticality: An explanation of the 1/f noise. *Phys. Rev. Lett.*, 59:381–384, Jul 1987. doi:10.1103/PhysRevLett.59.381.

[2] P. Bak, C. Tang, and K. Wiesenfeld. Self-organized criticality. *Phys. Rev. A*, 38:364–374, Jul 1988. doi:10.1103/PhysRevA.38.364.

[3] H. F. Chau and K. S. Cheng. Generalized sandpile model and the characterization of the existence of self-organized criticality. *Phys. Rev. A*, 44:6233–6240, Nov 1991. doi:10.1103/PhysRevA.44.6233.

[4] D. Dhar. Self-organized critical state of sandpile automaton models. *Phys. Rev. Lett.*, 64:1613–1616, Apr 1990. doi:10.1103/PhysRevLett.64.1613.

[5] D. Dhar. The abelian sandpile and related models. *Physica A: Statistical Mechanics and its Applications*, 263(1-4):425, Feb 1999. ISSN 0378-4371. doi:10.1016/s0378-4371(98)00493-2.

[6] D. Dhar. Some results and a conjecture for mannas stochastic sandpile model. *Physica A: Statistical Mechanics and its Applications*, 270(1-2):6981, Aug 1999. ISSN 0378-4371. doi:10.1016/s0378-4371(99)00149-1.

[7] D. Dhar and S. S. Manna. Inverse avalanches in the abelian sandpile model. *Phys. Rev. E*, 49:2684–2687, Apr 1994. doi:10.1103/PhysRevE.49.2684.

[8] A. A. Járai. Sandpile models. *Probab. Surveys*, 15:243–306, 2018. doi:10.1214/14-PS228. URL `https://doi.org/10.1214/14-PS228`.

[9] A. A. Járai, F. Redig, and E. Saada. Approaching criticality via the zero dissipation limit in the abelian avalanche model. *Journal of Statistical Physics*, 159(6):1369–1407, Jun 2015. ISSN 1572-9613. doi:10.1007/s10955-015-1231-z.

[10] L. Levine, W. Pegden, and C. Smart. Apollonian structure in the abelian sandpile. *Geometric and Functional Analysis*, 26: 306–336, 2012.

[11] S. Manna. Critical exponents of the sand pile models in two dimensions. *Physica A: Statistical Mechanics and its Applications*, 179(2):249 – 268, 1991. ISSN 0378-4371. doi:10.1016/0378-4371(91)90063-I.

[12] S. S. Manna. Two-state model of self-organized criticality. *Journal of Physics A: Mathematical and General*, 24(7):L363–L369, apr 1991. doi:10.1088/0305-4470/24/7/009.

[13] S. S. Manna. Sandpile models of self-organized criticality. *Current Science*, 77(3):388–393, 1999. ISSN 00113891.

[14] J.-F. Marckert, T. Selig, and Y.-B. Chan. A natural stochastic extension of the sandpile model on a graph. *Journal of Combinatorial Theory, Series A*, 120(7):1913–1928, 2013. URL `https://hal.archives-ouvertes.fr/hal-00919199`.

[15] E. Milshtein, O. Biham, and S. Solomon. Universality classes in isotropic, abelian, and non-abelian sandpile models. *Phys. Rev. E*, 58:303–310, Jul 1998. doi:10.1103/PhysRevE.58.303.

[16] W. Pegden and C. K. Smart. Convergence of the abelian sandpile. *Duke Mathematical Journal*, 162(4):627642, Mar 2013. ISSN 0012-7094. doi:10.1215/00127094-2079677.

[17] C. Tang and P. Bak. Critical exponents and scaling relations for self-organized critical phenomena. *Phys. Rev. Lett.*, 60: 2347–2350, Jun 1988. doi:10.1103/PhysRevLett.60.2347.